Radiological Evaluation of Newly Diagnosed Non-Brainstem Pediatric High-Grade Glioma in the HERBY Phase II Trial

Daniel Rodriguez Gutierrez[1,2], Chris Jones[3], Pascale Varlet[4], Alan Mackay[3], Daniel Warren[5], Monika Warmuth-Metz[6], Esther Sánchez Aliaga[7], Raphael Calmon[8], Darren R. Hargrave[9], Adela Cañete[10], Maura Massimino[11], Amedeo A. Azizi[12], Marie-Cécile Le Deley[13], Frank Saran[14], Raphael F. Rousseau[15], Gudrun Zahlmann[15], Josep Garcia[15], Gilles Vassal[13], Jacques Grill[13], Paul S. Morgan[1,2], and Tim Jaspan[16]

ABSTRACT

Background: The HERBY trial evaluated the benefit of the addition of the antiangiogenic agent Bevacizumab (BEV) to radiotherapy/temozolomide (RT/TMZ) in pediatric patients with newly diagnosed non-brainstem high-grade glioma (HGG). The work presented here aims to correlate imaging characteristics and outcome measures with pathologic and molecular data.

Methods: Radiological, pathologic, and molecular data were correlated with trial clinical information to retrospectively re-evaluate event-free survival (EFS) and overall survival (OS).

Results: One-hundred thirteen patients were randomized to the RT/TMZ arm ($n = 54$) or the RT/TMZ+BEV (BEV arm; $n = 59$). The tumor arose in the cerebral hemispheres in 68 patients (Cerebral group) and a midline location in 45 cases (Midline group). Pathologic diagnosis was available in all cases and molecular data in 86 of 113. H3 K27M histone mutations were present in 23 of 32 Midline cases and H3 G34R/V mutations in 7 of 54 Cerebral cases. Total/near-total resection occurred in 44 of 68 (65%) Cerebral cases but in only 5 of 45 (11%) Midline cases ($P < 0.05$). Leptomeningeal metastases (27 cases, 13 with subependymal spread) at relapse were more frequent in Midline (17/45) than in Cerebral tumors (10/68, $P < 0.05$). Mean OS (14.1 months) and EFS (9.0 months) in Midline tumors were significantly lower than mean OS (20.7 months) and EFS (14.9 months) in Cerebral tumors ($P < 0.05$). Pseudoprogression occurred in 8 of 111 (6.2%) cases.

Conclusions: This study has shown that the poor outcome of midline tumors (compared with cerebral) may be related to (1) lesser surgical resection, (2) H3 K27M histone mutations, and (3) higher leptomeningeal dissemination.

[1]Medical Physics and Clinical Engineering, Nottingham University Hospital Trust, Nottingham, United Kingdom. [2]Division of Clinical Neuroscience, University of Nottingham, Nottingham, United Kingdom. [3]Divisions of Molecular Pathology and Cancer Therapeutics, The Institute of Cancer Research, London, United Kingdom. [4]Anatomie et cytologie pathologiques, Centre Hospitalier Sainte Anne, Paris, France. [5]Department of Radiology, Leeds Teaching Hospitals, Leeds, United Kingdom. [6]Institute for Diagnostic and Interventional Neuroradiology, Würzburg University, Würzburg, Germany. [7]Department of Radiology and Nuclear Medicine, VU University Medical Center, Amsterdam, the Netherlands. [8]Pediatric Radiology, Necker Enfants Malades Hospital, Assistance Publique-Hôpitaux de Paris, Paris, France. [9]Haematology and Oncology Department, Great Ormond Street Hospital, London, United Kingdom. [10]Pediatric Oncology and Hematology Unit, Hospital La Fe, Valencia, Spain. [11]Pediatric Oncology Unit, Fondazione IRCCS Istituto Nazionale dei Tumori, Milan, Italy. [12]Division of Neonatology, Pediatric Intensive Care and Neuropediatrics, Medical University of Vienna, Vienna, Austria. [13]Pediatric and Adolescent Oncology and Unite Mixte de Recherche, Gustave Roussy, Université Paris-Saclay, Université Paris-Sud, Villejuif, France. [14]Neuro-oncology Unit, Royal Marsden Hospital, London, United Kingdom. [15]F. Hoffmann-La Roche, Basel, Switzerland. [16]Department of Radiology, Nottingham University Hospital Trust, Nottingham, United Kingdom.

Introduction

The HERBY trial was a phase II, open-label, randomized, multicenter study comparing the benefit of adding the antiangiogenic agent Bevacizumab (BEV arm) to conventional radiotherapy (RT) and Temozolomide (TMZ; RT/TMZ arm) in children between 3 and 18 years of age presenting with newly diagnosed, non-brainstem high-grade gliomas (HGG). Patients were recruited from 51 sites in 14 countries. The primary measures of response were overall survival (OS) and event-free survival (EFS) after 12 months; the study outcomes were recently published, demonstrating no overall advantage conferred by the addition of Bevacizumab (1).

HGGs are one of the most common malignant primary neoplasms of the pediatric central nervous system, occurring with a frequency of approximately 0.85 per 100,000 (2). These tumors were thought to be similar to HGG occurring in adults; however, molecular, genetic, and biological data now show that they are phenotypically distinct neoplasms (3). Greater understanding of their biology offers the potential for a more tailored approach to treatment, particularly employing novel therapeutic techniques targeting molecular and genetic pathways.

The need for expert neuropathological review within the context of a multicenter study is highlighted by the increasing understanding of the role played by the central midline location of a subset of pediatric HGGs (4).

The imaging appearances of HGG are best evaluated by MRI, which most accurately defines the anatomical localization, tumor margins, enhancement characteristics, and associated mass effect. Advanced MRI techniques offer the potential for a more "biological" noninvasive evaluation of these tumors; diffusion-weighted imaging provides

Translational Relevance

This article presents an evaluation of the radiological imaging of the HERBY study, which is combined with molecular and pathologic tumor characterization. This represents a more detailed *post hoc* analysis than undertaken in the recently published results of the primary study endpoints: safety and event-free survival. In-depth assessment of the heterogeneous nature of pediatric high-grade glioma (HGG) employing all three modalities underlines the importance of anatomical localization, surgical resectability, chemoradiotherapeutic response prediction and stratification, incidence of leptomeningeal (and subependymal) dissemination, and pseudoprogression. Distinctive imaging features of diffuse midline gliomas associated with H3 K27M mutations are described and contrasted with other midline and cerebral hemispheric pediatric HGGs. This study provides important information to help define response assessment in neuro-oncology specific to pediatric HGG.

information regarding cellular density, whereas perfusion-weighted imaging techniques enable assessment of tumor angiogenesis and capillary permeability. The metabolic profile of these tumors is also increasingly evaluated using magnetic resonance spectroscopy (5, 6). Although still regarded as investigational tools, these techniques are increasingly used in routine clinical practice.

Long-term survival in children with these tumors remains poor; median survival in studies ranges from 9 to 15 months (7). Recent progress in this field has been directed toward increasing recognition of the biological diversity of these tumors, their molecular profiling, and differential response to therapeutic interventions reflecting tumor subsets ranging from more benign phenotypes resembling low-grade gliomas to highly aggressive lesions with bleak outcomes, such as seen in diffuse intrinsic pontine gliomas (4, 8–10). Imaging remains an integral component in the diagnosis and characterization of these tumors as well as monitoring the response to a range of therapeutic interventions employed in their treatment.

The primary outcome measures (EFS and OS) of the study were evaluated using standard structural and multimodal MRI techniques. Combining imaging with the main molecular genetic and consensus histopathologic evaluations offers the potential to improve and enhance the management of these tumors, and formed the basis for the secondary research aims of the HERBY trial. Initial work to address this combination has recently been published with the focus on the molecular analysis (11). This work expands on the radiological characterizations of the patients, focusing on:

- Retrospective re-evaluation of and identification of additional radiological markers.
- Preoperative radiological characterizations correlated with molecular genetics and histopathology.
- Evolution of radiological characteristics related to response, correlated with the baseline genetic and histopathologic morphology.

Materials and Methods

The HERBY trial was conducted as part of a pediatric investigation plan. The protocol was approved by the applicable independent ethics committees and Institutional Review Boards, and the study was conducted in accordance with applicable regulations, International Council for Harmonisation of Technical Requirements for Pharmaceuticals for Human Use Good Clinical Practice guidelines, and the ethical principles enshrined in the Declaration of Helsinki. Written-informed consent was obtained from the patient/parents or legally acceptable representatives prior to enrolment; consent was also obtained prior to collection of tissue for the exploratory biomarker analyses.

This article addresses the initial intention-to-treat cohort ($n = 121$) of patients aged between 3 and 18 years who entered the HERBY trial between October 2011 and February 2015. All patients underwent expert neuropathological consensus review prior to entering the trial. Exclusion criteria included: metastatic disease at study entry, previously treated HGG, diffuse tumors such as gliomatosis cerebri, tumors arising centrally within the pons, anaplastic ganglioglioma, and pleomorphic xanthoastrocytoma (PXA).

Imaging

Radiological imaging was undertaken on all patients preoperatively. In some cases from secondary sites, preoperative imaging was not available for analysis, but some imaging characteristics (tumor site epicenter, lesion definition, and degree or absence of perilesional edema) could still be derived from the immediate and early postoperative imaging. All postoperative imaging was undertaken according to the previously published imaging protocol (12). Tumor response evaluation was undertaken according to the Response Assessment in Neuro-Oncology (RANO) criteria (13) by a panel of five experienced pediatric neuroradiologists for each timepoint (14).

To add value to the RANO evaluation required by the HERBY trial, *post hoc* radiological analysis was undertaken to evaluate additional preoperative MRI characteristics that were not predicated in the main HERBY assessment: epicenter location, necrosis/cysts, hemorrhage, tumor margin definition (well-defined, ill-defined, or ill-defined–multifocal), contrast enhancement characteristics (strong, strong-focal, moderate, minor, none), and perilesional edema (severe, moderate, minor, none). Preoperative tumor volumes and apparent diffusion coefficient (ADC) values were also analyzed. Extent of resection was assessed according to a simplified version of the Vasari criteria (ref. 15; total or near total tumor resection, >95%; major debulking, >50% and <95%; minor debulking, <50% resection; biopsy). In patients with no or minimally enhancing tumor, extent of resection was determined by the absence of tissue on the preoperative imaging that was identifiable as most likely to be tumoral on the basis of all imaging sequences available. In addition, the following postoperative measures were recorded: presence/absence and location of any leptomeningeal (or subependymal) metastatic (LMM) dissemination, pseudoprogression, or pseudoresponse (psPD/psPR). For a more detailed description of the recorded metrics, see Supplementary Materials: Image Analysis Methodology.

Pathology

All patients in the main HERBY trial underwent a real-time prerandomized screening by a central neuropathologist employing; *post hoc* analysis of the tumor histology was undertaken by six experienced neuropathologists, with reference to 2007 World Health Organization (WHO) classification (1). Due to the newly defined entity diffuse midline glioma (DMG) grade IV, H3F3A K27M-mutant, introduced in the WHO 2016 (16) classification, the WHO 2007 grade was updated based on the combined presence of H3F3A K27M mutation and midline location defined by imaging (i.e., midline-located, H3F3A K27M-mutated diffuse grade III gliomas regraded as

WHO 2016 grade IV). The statistical analyses were performed primarily using the WHO 2007 grade classification and secondarily using the updated data.

Biology

Specimens from 89 of the patients who consented to exploratory translational research were collected and underwent Sanger sequencing for H3F3A, Illumina 450K BeadArray methylation profiling, whole exome sequencing, capture-based fusion panel sequencing, and RNA sequencing (11).

Statistical analysis

Statistical analysis was performed using IBM SPSS Statistics for Windows, version 25 (IBM Corp.). Univariate relationships between nominal characteristics were compared using χ^2 tests. Univariate ordinal labels and numeric metrics were compared using Mann–Whitney (MW) and Kruskal–Wallis (KW) tests. Univariate differences in survival were analyzed by the Kaplan–Meier (KM) method and significance determined by the log-rank test in Matlab, Release 2017 (The MathWorks Inc.). All tests were two-sided, and a P value of less than 0.05 was considered significant.

Results

Of the initial 121 patients, 5 withdrew from the trial after randomization (withdrawn consent = 4, failed to meet eligibility criteria = 1). Following *post hoc* pathologic analysis, three cases were reclassified as non-HGG tumors (oligodendroglioma grade II, $n = 1$; anaplastic ganglioglioma, $n = 2$). The age range of the 113 patients who remained on study was 3.1 to 17.8 years (mean, 10.8 years). Sixty-seven (59%) patients were male, and 46 (41%) female. Following *post hoc* radiological analysis, the site of tumor origin was designated as arising within the cerebral hemispheres (Cerebral group) in 68 (60%) patients and in a midline location (Midline group) in 45 (40%). A heatmap of the distribution of the epicenters can be seen in **Fig. 1**. Supplementary Table S1 provides details of the complete data set

analyzed. Supplementary Table S2 summarizes the demographics associated with the major mutation and methylation subclass entities. Following *post hoc* central neuropathology review and integration with molecular data, the tumors were given a final histologic consensus classification of astrocytoma (93%, 105/113), HGG Not Otherwise Specified (NOS; 4%, 5/113), and oligoastrocytomas (3%, 3/113). After consensus review, 81% (92/113) had grade IV tumors and 19% (21/113) grade III tumors.

Radiological features

The study demographics related to treatment arm, tumor grade, and major mutations for the whole study cohort is recorded in **Table 1**. **Table 2** details imaging features according to location and mutation status; Supplementary Fig. S1 details their features associated with tumor grade and Supplementary Fig. S2 with histone status.

Enhancement, radiological necrosis, hemorrhage, tumor volumes, and ADC values

Location

In the Cerebral group, 40 of 55 (73%) showed moderate/strong tumor enhancement, whereas 15 of 55 (27%) had minor/no enhancement. Necrosis was present in 42 of 55 (76%) cases, and hemorrhage in 27 of 55 (49%) cases (all associated with necrosis). In the Midline group, 26 of 43 (60%) showed moderate/strong enhancement, with minor/no enhancement in 17 of 43 (40%). Necrosis was present in 30 of 43 (70%), and hemorrhage in 13 of 43 (30%), associated with necrosis in 12 of 13. None of the above metrics were significantly different depending on location, nor were the ADC values, but Cerebral tumors had larger T2-weighted abnormalities (MW U = 260.0, $P < 0.05$), and enhancing volumes (MW U = 426.0, $P < 0.05$).

Tumor grade

Grade IV: In 63 of 81 (78%) patients, the tumors showed moderate/strong enhancement, with minor/no enhancement in 14 of 81 (17%)
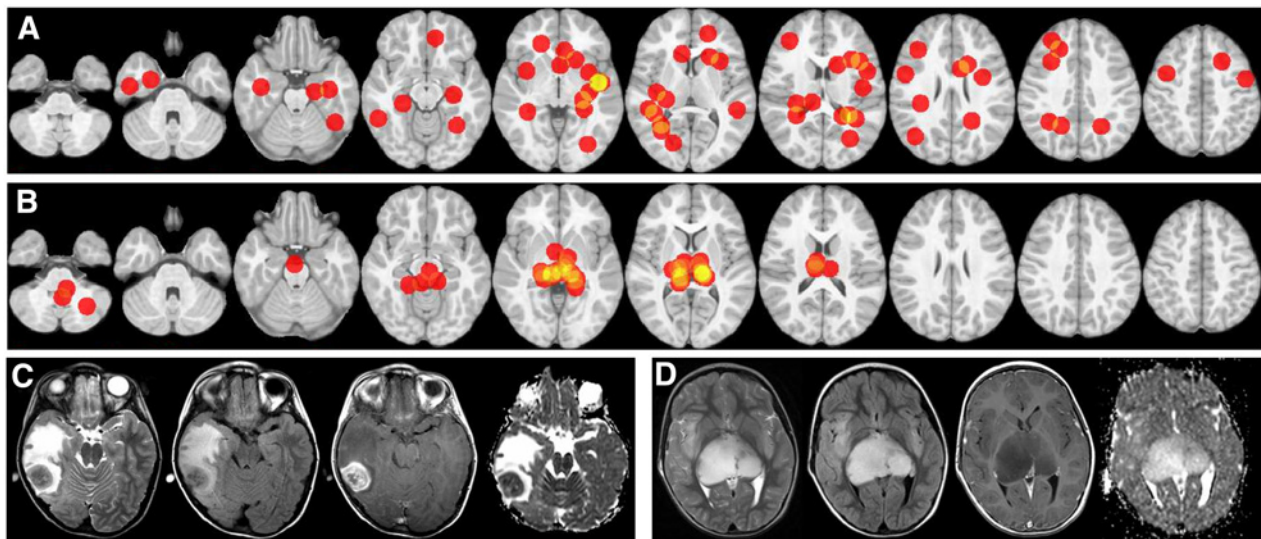

Figure 1.
Location and examples of typical pediatric HGGs in the HERBY study. Epicenter heatmaps of Cerebral (**A**) and Midline (**B**) tumors overlaid on a standardized T1-weighted pediatric brain. Exemplar sequences: T2-weighted, Fluid-attenuated inversion recovery (FLAIR), contrast enhanced T1-weighted, and ADC of a Cerebral tumor (**C**) and a Midline tumor (**D**).

Table 1. Patient baseline characteristics of the study population.

	RT/TMZ $n = 54$	BEV+RT/TMZ $n = 59$	Total $n = 113$
WHO grade HGG[a], n (%)			
III	11 (20)	10 (17)	21 (19)
IV	43 (80)	49 (83)	92 (81)
Histone mutation status, n (%)			
WT	30 (55)	26 (44)	56 (50)
H3 G34R	5 (9)	2 (3)	7 (6)
H3 K27M	9 (17)	14 (24)	23 (20)
Missing	10 (19)	17 (29)	27 (24)
Location of HGG, n (%)			
Midline	20 (37)	25 (42)	45 (40)
Cerebral	34 (63)	34 (58)	68 (60)

[a]Stratification factor for randomization.

cases. Necrosis was present in 69 of 81 (85%) cases. Intratumoral hemorrhage was present in 38 of 81 (48%) cases.

Grade III: Moderate/strong enhancement was present in 3 of 17 (18%) cases, and minor/no enhancement in 14 of 17 (82%) cases. These enhancement patterns were significantly different to grade IV tumors (MW U = 1513.0, $P < 0.05$). Although radiological tumor necrosis was present in 3 of 17 (18%) cases, and the incidence was significantly lower than grade IV tumors, χ^2 (1, $N = 98$) = 32.8, $P < 0.05$. In 1 Midline case (right thalamic WT tumor), it was associated with moderate ring enhancement (Supplementary Fig. S3) and in two Cerebral cases with minor ring enhancement (Supplementary Fig. S4). In these cases, the presence of necrosis did not correlate with the histologic grading. Intratumoral hemorrhage was present in 1 of 17 (13%) cases, which was associated with necrosis, being significantly different to grade IV cases, χ^2 (1, $N = 99$) = 10.4, $P < 0.05$. Although the ADC values of grade III tumors were not significantly different to grade IV's, the sizes of the T2-weighted abnormalities were smaller (MW U = 571.0, $P < 0.05$), necrosis and cysts were more infrequent (MW U = 1513.0, $P < 0.05$), and the size of the enhancing component relative to the overall tumor volume was smaller (MW U = 709.0, $P < 0.05$) in grade III's.

Histone mutational status

H3 wild type: Twenty-seven of 35 (77%) Cerebral cases showed moderate/strong enhancement compared with 3 of 9 (33%) Midline tumors χ^2 (1, $N = 43$) = 5.1, $P < 0.05$. Cerebral wild-type (WT) tumors also showed a higher incidence of necrosis [77% (27/35)] and hemorrhage [54% (19/35)] compared with Midline WT tumors [55% (5/9) and 22% (2/9)].

DMG H3 K27M–mutant: These tumors were generally strongly enhancing and occurred in older patients (Supplementary Fig. S5). Fourteen of 22 (64%) cases with preoperative imaging showed moderate/strong enhancement, with radiological necrosis in 15 of 22 (68%) and hemorrhage in 6 of 22 (27%). Compared with Midline WT tumors, H3 K27M–mutant tumors showed more enhancement (Mann–Whitney U = 49.0, $P < 0.05$). This was irrespective of tumor grade (13/22 Grade IV H3 K27M–mutant vs. 3/9 Grade IV WT Midline tumors show moderate/strong enhancement). In 14 of 23 patients with H3 K27M–mutant tumors, tumor volumes, ratios, and ADC values

were not significantly different between H3 K27M–mutant and Midline WT tumors.

H3 G34R–mutant: These tumors were generally poorly enhancing, with only 2 of 6 (33%) with preoperative imaging available showing moderate/strong enhancement, and 4 of 6 (66%) necrosis and hemorrhage. Tumor volumes, ratios, and ADC values were not significantly different to other Cerebral WT tumors.

Methylation subclass and IDH class

The numbers of cases with defined methylation subclass and accompanying imaging were too few for useful evaluation except for cases with a methylation pattern similar to PXA (PXA-like) and Diffuse isocitrate dehydrogenase 1 (IDH1) mutants, which are described below:

- PXA-like: All showed strong enhancement, 8 of 9 (89%) necrosis and 4 of 9 (44%) hemorrhage.
- Diffuse IDH1-mutant: Both cases with available imaging showed no enhancement, necrosis, or hemorrhage.

Tumor definition and perilesional edema
Location

Tumor definition was comparable between Cerebral and Midline cases; 50 of 68 (74%) Cerebral tumors and 33 of 45 (73%) Midline tumors showed well-defined margins. Minor or absent perilesional edema was characteristic of Midline tumors (44/45—98%), with 1 case having moderate perilesional edema. In contrast, 46 of 68 (68%) Cerebral cases exhibited moderate or severe surrounding edema (MW U = 343.0, $P < 0.05$).

Tumor grade

In the 21 grade III cases, no/minor perilesional edema was present in 15 (71%), whereas 6 cases (29%) had moderate edema (all Cerebral cases). Of the 92 grade IV patients, 51 (55%) had no/minor edema, and 41 moderate/severe edema (45%). Grade IV tumors were significantly more well-defined (72/92, 78%), χ^2 (1, $N = 113$) = 6.7, $P < 0.05$, and had more moderate/severe edema (41/92, 45%) when compared with grade III's (well defined = 11/21, 52%; moderate edema = 6/21, 29%; MW U = 1374.0, $P < 0.05$), which was also reflected in a significantly smaller tumor-to-T2–weighted abnormality ratio (MW U = 205.0, $P < 0.05$).

Histone mutational status

H3 WT: Perilesional edema was absent/minor in 25 (45%) patients (16 Cerebral, 9 Midline) and moderate/severe in 31 (55%) patients, all in the Cerebral group.

DMG H3 K27M–mutant: Tumors were well defined in 20 of 23 patients; perilesional edema was either absent in or minor in all cases.

Midline WT cases: Tumor definition and perilesional edema were similar to the H3 K27M–mutant Midline tumors.

H3 G34R–mutant: Only 2 of 7 (29%) cases were well-defined; 5 of 7 (71%) were ill-defined. Compared with Cerebral WT (5/47) tumors, tumor definition for H3 G34R mutants was significantly different, χ^2 (1, $N = 51$) = 5.1, $P < 0.05$, and they were mostly multicentric (discontinuous multilobar or extensively diffuse multilobar tumors; 5/7), χ^2 (1, $N = 54$) = 14.9, $P < 0.05$ (Supplementary Fig. S6).

Table 2. Baseline imaging characteristics related to location and major biomolecular classes ($n = 113$).

Tumor location Major mutations and methylation subclasses	Enhancement	Necrosis	Hemorrhage	Tumor definition	Perilesional edema
Cerebral $n = 68$	Strong = 36 Moderate = 4 Minor/none = 15 NA = 13	Yes = 42 No = 13 NA = 13	Yes = 27 No = 28 NA = 13	Well-defined = 50 Ill-defined/diffuse = 18	None = 8 Minor = 14 Moderate = 36 Severe = 10
Midline $n = 45$	Strong = 25 Moderate = 1 Minor/none = 17 NA = 2	Yes = 30 No = 13 NA = 2	Yes = 13 No = 30 NA = 2	Well-defined = 33 Ill-defined/diffuse = 12	None = 21 Minor = 23 Moderate = 1 Severe = 0
Cerebral WT $n = 47$	Strong = 26 Moderate = 1 Minor/none = 8 NA = 12	Yes = 27 No = 8 NA = 12	Yes = 19 No = 16 NA = 12	Well-defined = 38 Ill-defined/diffuse = 9	None = 6 Minor = 10 Moderate = 26 Severe = 5
Midline WT $n = 9$	Strong = 3 Minor/none = 6	Yes = 5 No = 4	Yes = 2 No = 7	Well-defined = 5 Ill-defined/diffuse = 4	None = 5 Minor = 4 Moderate = 0 Severe = 0
H3 K27M $n = 23$	Strong = 14 Moderate = 1 Minor/none = 7 NA = 1	Yes = 16 No = 6 NA = 1	Yes = 7 No = 15 NA = 1	Well-defined = 19 Ill-defined/diffuse = 4	None = 10 Minor = 13 Moderate = 0 Severe = 0
H3 G34 $n = 7$	Strong = 1 Moderate = 1 Minor/none = 4 NA = 1	Yes = 4 No = 2 NA = 1	Yes = 4 No = 2 NA = 1	Well-defined = 2 Ill-defined/diffuse = 5	None = 1 Minor = 3 Moderate = 2 Severe = 1
PXA-like $n = 9$	Strong = 9	Yes = 8 No = 1	Yes = 4 No = 5	Well-defined = 8 Ill-defined/diffuse = 1	None = 0 Minor = 2 Moderate = 5 Severe = 2
IDH1 $n = 4$	None = 3 NA = 1	Yes = 1 No = 2 NA = 1	No = 3 NA = 1	Well-defined = 4	None = 1 Minor = 2 Moderate = 1 Severe = 0
LGG-like $n = 2$	Strong = 1 NA = 1	Yes = 1 NA = 1	No = 1 NA = 1	Well-defined = 2	None = 1 Moderate = 1

Abbreviations: LGG, low-grade glioma; NA, not available.

Perilesional edema was absent/minor in 4 of 7, moderate in 2 of 7, and severe in 1 of 7 H3 G34R–mutant cases.

Methylation subclass and IDH class

PXA-like: Eight of 9 (89%) of PXA-like tumors were well-defined. Perilesional edema was absent/minor in 2 of 9 and moderate/severe in 7 of 9. All 4 patients with IDH1 mutations had diffuse, ill-defined tumors, with no/minor perilesional edema in 3 of 4.

Extent of surgical resection

Resection rates per treatment arm for the 113 patients in the study are given in Supplementary Table S5 and according to tumor grade in Supplementary Table S6. Total/near-total resection (NTR) occurred in 49 (43%) patients; 32 (28%) had major tumor debulking, 12 (11%) minor debulking, and 20 (18%) biopsy only.

The extent of total/NTR in the Cerebral group (65%) was significantly higher than in the Midline group (11%), MW U = 529.00, $P < 0.05$, with lower rates of minor debulking (3% vs. 22%) and biopsy (6% vs. 36%), see Supplementary Fig. S7. There was a significantly higher total/NTR rate in grade IV tumors [42/92 (45%)] than for grade III tumors [7/21 (33%)], $\chi^2 (1, N = 113) = 5.36, P < 0.05$.

Leptomeningeal dissemination

LMM dissemination occurred in 27 patients. Whole neuraxial imaging was available in 21 of 27 (spinal MRI unavailable in 6/27), the imaging features of which are documented in Supplementary Table S5. Supratentorial LMM was present in 16 of 27, infratentorial LMM in 17 of 27, and spinal LMM in 15 of 21 (in 6 patients, the spine
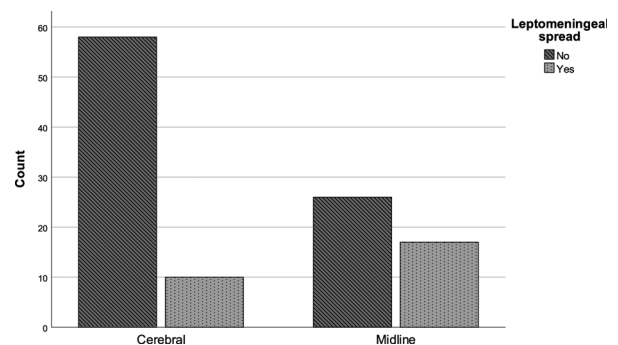

Figure 2.
Incidence of leptomeningeal spread in Cerebral versus Midline tumors.

was the only involved site). LMM occurred more frequently, χ^2 (1, $N = 111) = 8.82$, $P < 0.05$, in patients with Midline tumors (17/43, 40%) than Cerebral tumors (10/68, 15%), see **Fig. 2**. In 6 of 17 (35.3%) Midline cases with preoperative imaging, the primary lesion showed minor or no enhancement (an example can be seen in Supplementary Fig. S8). In contrast, the primary tumor showed strong enhancement in all 8 (100%) patients with LMM who had Cerebral tumors with preoperative imaging available.
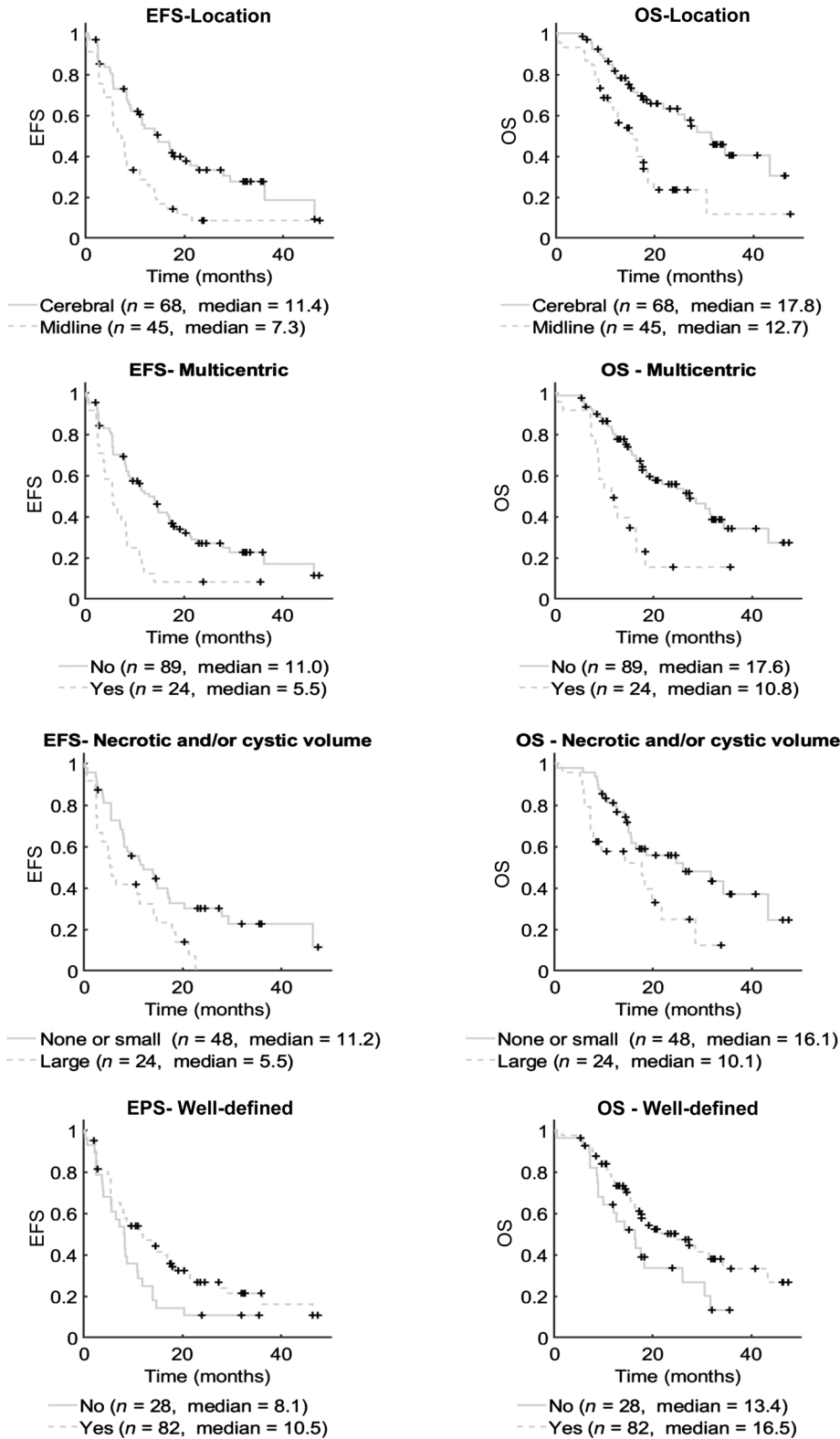

Figure 3.
Radiological characteristics resulting in statistically significant differences (log rank $P < 0.05$) in EFS and OS.

All 9 Cerebral cases with LMM underwent major/GTR; however, LMM occurred in 55% (10/18) of Midline cases where there had been major/GTR, indicating that extent of resection did not have a substantial impact upon the incidence of LMM.

In 11 of 17 of all the Midline cases with LMM, leptomeningeal disease occurred in the presence of stable primary tumor; in 6 of 17 cases, there was concurrent local progression and distant leptomeningeal spread. In 5 of 10 Cerebral cases, LMM occurred in the presence of stable local disease; local progression and LMM occurred concurrently in 5 of 10 cases. In total, 16 of 27 (59%) cases displayed LMM disease in the presence of local tumor control.

There was no statistical difference in incidence of LMM between treatment arms, occurring in 15 of 27 (56%) patients in the RT/TMZ arm (15/27—56%) and 12 of 27 (44%) in the BEV arm. LMM occurred in 8 of 23 (35%) patients with an H3 K27M mutation (4 in each treatment arm), in 14 of 56 (25%) patients with WT mutations (10 in the RT/TMZ arm and 4 in the BEV arm), and in 1 of 7 patient with an H3 G34 mutation (RT/TMZ arm). Four patients with LMM had no tissue sample available for molecular assessment. Of the 13 Midline tumor cases with LMM that had molecular data available, 8 of 13 (62%) had H3 K27M mutations (4 in each treatment arm) and 5 of 13 (38%) WT mutations (all in the RT/TMZ arm).

Pseudoprogression and pseudoresponse

Pseudoprogression occurred in 8 of 111 (7%) cases (2 patients died early in the treatment and had no imaging), 5 in the RT/TMZ arm (for an example, see Supplementary Fig. S9), and in 3 cases in the BEV arm, χ^2 (1, $N = 111$) = 0.75, $P = 0.39$. psPD was present in 6 of 68 in the Cerebral group and 2 of 45 in the Midline group. In the Cerebral group, four had lobar tumors [1 with an H3 G34 mutation, 3 with WT mutations (1 with PXA-like methylation subtype)], and two diffuse multicentric tumors (1 with an H3 G34 mutation, no molecular data on the second). In the Midline group, 2 patients had H3F3A K27M mutations, one unithalamic and one a diffuse bithalamic tumor. In those patients with MGMT gene promoter status available, 5 were unmethylated, whereas 1 was methylated (2 had no biological samples). There were no cases of pseudoresponse in the study cohort.

Outcomes measures

Midline tumors had significantly shorter EFS (median 7.3 vs. 11.4 months, log-rank $P <0.05$) and OS (median 12.7 vs. 17.8 months, log-rank $P < 0.05$) than Cerebral tumors. H3 K27M–mutant tumors showed no distinct survival characteristics compared with WT Midline tumors (Supplementary Fig. S10). Diffusely infiltrative or multilobar tumors had significantly shorter EFS (median 5.5 vs. 11.0 months, log-rank < 0.05) and OS (median 10.8 vs. 17.6 months, log-rank < 0.05), as did those with LMM (EFS median 4.4 vs. 13.4 months, log-rank $P < 0.05$; OS median 9.0 vs. 18.4 months, log-rank $P < 0.05$). Well-defined tumors had significantly longer EFS (median 10.5 vs. 8.1 months, log-rank $P < 0.05$) and OS (median 16.5 vs. 13.4 months, log-rank $P < 0.05$). Tumors with large (>median size) cystic and/or necrotic components had significantly shorter EFS (median 5.5 vs. 11.2 months, log-rank $P < 0.05$) and OS (median 10.1 vs. 16.1 months, log-rank $P < 0.05$) than those with small or no cysts/necrotic areas. KM curves for these groups can be seen in Fig. 3. There was no significant difference in EFS or OS related to the size of the overall abnormality, whole tumor or enhancement volumes, or in relation to average and minimum ADC values. Both EFS and OS were longer for patients with psPD than for those without, but these were not significantly different.

Extent of surgical resection

Supplementary Fig. S11 indicates the EFS and OS outcomes for Total/NTR compared with minor debulk, major debulk, and biopsy only. Although there was no significant difference in outcome between patients undergoing major compared with minor tumor debulking (EFS log-rank $P = 0.69$, OS $P = 0.84$), there was a significant difference between major debulk and total/NTR (EFS log-rank $P <0.05$; OS log-rank $P < 0.05$; see Fig. 4). There was no significant difference between treatment arms and type of resection, MW U = 1492.00, $P = 0.27$.
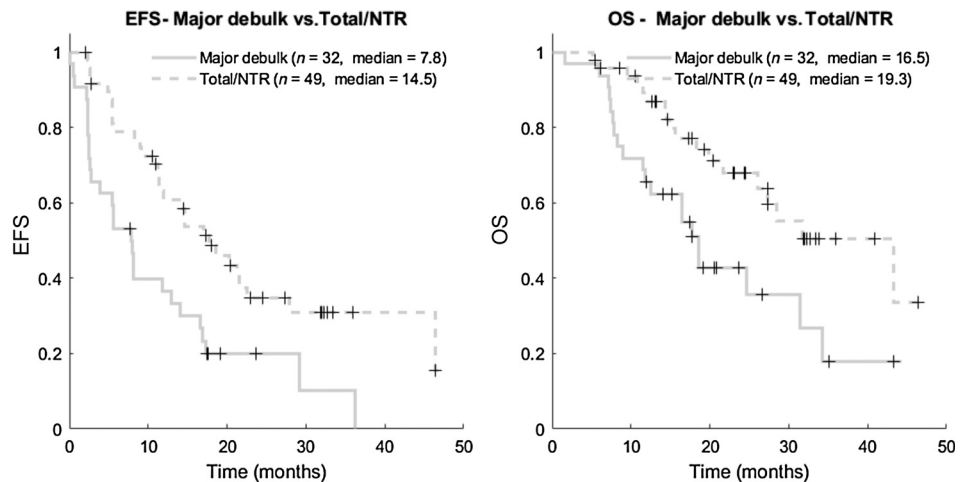
Anatomical location

Supplementary Table S6 details the outcome for Cerebral and Midline location tumors according to treatment arm, with more precise locations for Cerebral cases in Supplementary Table S7 and Midline in Supplementary Table S8.

Tumor grade

Supplementary Table S9 displays the outcomes related to tumor grade. There was no significant difference between grade III and grade IV tumors (mean EFS 15.7 vs. 11.8 months, log-rank $P = 0.36$; mean OS 19.3 vs. 17.8 months, log-rank $P = 0.85$). There was a significant difference in EFS between Cerebral grade III and grade IV (mean

Figure 4.

Survival curves of EFS and OS of Major debulk vs. Total/NTR: In both cases, they are significantly different, log-rank $P < 0.05$.

EFS- Major debulk vs.Total/NTR

Major debulk ($n = 32$, median = 7.8)
Total/NTR ($n = 49$, median = 14.5)

OS - Major debulk vs. Total/NTR

Major debulk ($n = 32$, median = 16.5)
Total/NTR ($n = 49$, median = 19.3)

EFS = 19.5 vs. 13.8 months, log-rank $P < 0.05$), but not in the Midline group (mean EFS = 9.6 and 8.9 months, log-rank $P = 0.19$). Differences in OS were not significant.

Treatment arm

As previously reported (1), there was no significant difference in outcome between the BEV and the RT/TMZ arms. Adjusting for location, there were no differences in either EFS (Cerebral RT/TMZ median EFS = 14.0 vs. BEV 14.6 months and Midline RT/TMZ median EFS = 7.9 vs. BEV 6.4 months, log-rank $P = 0.51$) or OS (Cerebral RT/TMZ median OS = 31.7 vs. BEV 31.4 months and Midline RT/TMZ median OS = 14.2 vs. BEV 15.5 months, log-rank $P = 0.74$).

Leptomeningeal disease

Outcomes for patients with LMM are provided in Supplementary Table S10, and KM curves for patients with and without leptomeningeal disease are given in Supplementary Fig. S12. Compared with local recurrence/progression cases only, patients with LMM had significantly shorter EFS (mean 5.2 vs. 12.5 months) and OS (median 10.7 vs. 27.0 months), log-rank $P < 0.05$. There were no differences in survival after adjusting for treatment arm.

Discussion

The HERBY study is one of the largest multicenter, multinational phase II–randomized trials of pediatric HGGs undertaken. The primary outcome measures were drug safety, OS, and EFS as defined by RANO. The trial opened in 2011, prior to the development of radiological response assessment criteria, the discovery of histone gene mutations (17, 18) and subsequent extensive genome sequencing (19, 20), and the WHO 2016 classification of a distinct entity of tumors defined as DMGs with H3 K27M mutation (16). The present study provides a more detailed analysis of the radiological findings following extended *post hoc* imaging analysis. There was a 40% incidence of radiologically defined Midline tumors. Tissue samples for mutation and methylation subclass evaluation were available in 32 of 45 (71%) patients with Midline tumor remaining on study, of whom 23 of 32 (72%) harbored H3 K27M mutations; none were present in the Cerebral Group, consistent with recently reported studies (16, 18, 21, 22). In contrast to the 2016 WHO descriptor of these tumors showing diffuse tumoral infiltration at a microscopic scale (23), in 78% (36/46) of cases the tumors were radiologically well-defined. Although the majority of patients with H3K27 M mutations showed strong enhancement, a substantial minority (9/23) were classified as grade III, of which 7 of 8 with preoperative imaging showed little or no enhancement. As the trial started prior to the publication of the current WHO criteria, these tumors would now be classified as grade IV. Aboian and colleagues (24) have previously performed a radiological comparison between H3 K27M–mutant and other midline WT tumors, including ADC values (25). Our findings generally agree with their results but for the significantly higher proportion of strongly enhancing H3 K27M mutants with respect to WTs in the HERBY cohort.

The OS and EFS of the Midline tumors were significantly shorter than for the Cerebral Group. For both groups, patients on the BEV arm had a lower incidence of MRI contrast enhancement of the recurrent/progressing tumor compared with those on the RT/TMZ arm, which may indicate a differential response to BEV of these tumors. The poorer outcome metrics of the Midline group likely reflects a combination of:

1 The high (72%) incidence of H3 K27M–mutant tumors identified in patients with Midline tumors who had biological material available for analysis
2 A significantly lower incidence of total/NTR reflecting the unfavorable surgical location of these tumors compared with Cerebral tumors
3 Higher incidence of leptomeningeal dissemination.

Regarding extent of tumor resection, defining tumor margins and degree of surgical excision, particularly with poorly or totally nonenhancing tumors, remains a radiological challenge. When tumors are diffused and ill-defined, the surgical margins become indistinct, limiting the ability to achieve a complete resection. Anatomical localization also determines the degree of resection possible, tumors involving midline structures being more surgically challenging. This is reflected by the lower proportion of total/NTR or major tumor debulking in Midline tumors (42%) compared with Cerebral tumors (91%). Although achieving total/NTR confers an OS benefit, the significant difference in OS and EFS between debulking (minor and major), as compared with total/NTR, supports the value of near-complete cytoreduction compared with any other form of surgery. These findings are in line with other studies (26–29) but are different to those reported in the main HERBY paper (1), where extent of resection was defined surgically, and suggested no significant differences debulking (minor or major) and total/NTR. The disagreement between the radiological and surgical criteria affected 19% of the patients in the HERBY study.

Although small in number, there did not appear to be a negative outcome effect of Midline tumors harboring an H3 K27M mutation compared with those with WT mutations. This result is different to that of Karremann and colleagues (30), who showed a clear poorer survival in H3 K27M mutants, although also including diffuse intrinsic pontine gliomas (DIPG). In addition, the poor survival in the HERBY cohort of the histone WT Midline cases compared with that of the H3 K27M–mutant group might possibly be explained by a substantially larger proportion of biopsies in the WT group. The radiological features and OS/EFS metrics of Midline tumor cases without molecular data were similar to those where H3 K27M mutations were present. With respect to tumor grade, there was a significant difference in OS and EFS between Cerebral and Midline tumors for both grade III and grade IV tumors, the poorer outcome of the Midline tumors reflected by the high proportion of H3 K27M–mutant tumors in this location as well as lower resection rates.

Radiological necrosis was identified by radiological imaging in 3 patients that were histopathologically assigned as grade III tumors. In two cases that had biopsy only (one bithalamic, one a diffuse left insular tumor), this apparent contradiction may have reflected surgical sampling of parts of the tumors that were not radiologically necrotic, possibly resulting in misgrading of these tumors. This may in turn have underestimated the difference in outcome metrics between grade III and grade IV tumors.

Pseudoprogression was identified in 8 of 111 (7.1%) of cases, 5 in the RT/TMZ arm and 3 in the BEV arm, which is lower than that reported in comparable adult HGG studies that report up to a 36% incidence (31). The survival benefit conferred by exhibiting psPD, although not meeting statistical significance, appears to mirror that reported in some studies of adult patients with GBM (32–34). Leptomeningeal and/or subependymal dissemination occurred in 24% of the study population, with a higher incidence in patients with Midline tumors (40%) compared with Cerebral tumors (15%). In contrast, the incidence in adult HGG studies is lower; Parsa and colleagues recorded

an incidence of 2.3% (ependymal and distant leptomeningeal) in 1,471 patients (35). In a smaller study in 1994, Arita and colleagues found 20 of 157 patients with HGGs with antemortem (myelographic) diagnosed leptomeningeal spread, although 7 occurred in patients < 19 years of age (36). Excluding patients with evidence of LMM at presentation, Dardis and colleagues identified 30 patients with LMM in a retrospective analysis of 12,477 patients (37). The reported incidence of LMM is higher in pediatric HGG. Wagner and colleagues found a 17% incidence of LMM in 256 patients < 20 years of age presenting with newly diagnosed HGG or DIPG identified on MRI (38), a similar proportion to the HERBY study. The higher incidence of Midline tumors in the HERBY study with LMM mirrors the high incidence of LMM in DIPG, which share a high incidence of H3 K27M mutations. Buczkowic and colleagues found LMM in 17 of 44 (38.6%) patients with DIPG who had an autopsy (39). It is possible that the incidence of LMM in patients recruited to the HERBY study would have been higher if autopsies had been undertaken in all nonsurviving children. The presence of LMM is an important factor in the assessment of tumor response to therapy, which is underrepresented in the the study's central radiological review committee criteria (spinal imaging and exclusion of LMM is not routinely undertaken in the adult context). *Post hoc* analysis revealed LMM at an earlier stage than detected by the study CRRC in several cases, reflecting the difficulty in identifying the earliest subtle features even within the context of an independent review process.

In conclusion, the HERBY study confirms the phenotypically distinct entity of Midline tumors that harbor a high incidence of H3 K27M mutations. Radiologically, these tumors are characterized by being well-defined with minimal or no perilesional edema in the vast majority of cases, and smaller tumor volumes at presentation, likely reflecting their central location. Regarding outcome metrics, OS and EFS of these tumors were significantly shorter than that of tumors arising in the Cerebral hemispheres (apart from the small number with H3 G34R mutations), highlighting the importance of considering these tumors separately in future prospective therapeutic interventional trials of pediatric HGGs. Midline tumors included a subset that uniquely harbored an H3 K27M histone mutation, had a lower total/NTR rate (42% vs. 91%), and had a higher incidence of leptomeningeal dissemination (38% vs. 15%). The universally worse prognosis of Midline tumors for both H3 K27M–mutant and WT histone mutants supports considering these tumors holistically when defining treatment paradigms, even when biological markers are not available.

The HERBY study has emphasized the heterogeneity of molecular findings, imaging, and response to therapy in pediatric HGGs. Incorporating leptomeningeal dissemination in future pediatric-focused response assessment criteria is stressed. The importance of determining a midline location and other related radiological characteristics of these tumors, which present a worse outcome than cerebral ones, should be considered when designing future therapeutic trials of pediatric HGGs.

References

1. Grill J, Massimino M, Bouffet E, Azizi AA, McCowage G, Cañete A, et al. Phase II, open-label, randomized, multicenter trial (HERBY) of bevacizumab in pediatric patients with newly diagnosed high-grade glioma. J Clin Oncol 2018;36:951–8.
2. Ostrom QT, Gittleman H, Fulop J, Liu M, Blanda R, Kromer C, et al. CBTRUS statistical report: primary brain and central nervous system tumors diagnosed in the united states in 2008–2012. Neuro Oncol 2015;17:iv1–62.
3. Jones C, Perryman L, Hargrave D. Paediatric and adult malignant glioma: close relatives or distant cousins? Nat Rev Clin Oncol 2012;9:400–13.
4. Eisenstat DD, Pollack IF, Demers A, Sapp MV, Lambert P, Weisfeld-Adams JD, et al. Impact of tumor location and pathological discordance on survival of children with midline high-grade gliomas treated on Children's Cancer Group high-grade glioma study CCG-945. J Neurooncol 2015;121:573–81.
5. Panigrahy A, Blüml S. Neuroimaging of pediatric brain tumors: from basic to advanced magnetic resonance imaging (MRI). J Child Neurol 2009;24:1343–65.
6. Wilson M, Cummins CL, MacPherson L, Sun Y, Natarajan K, Grundy RG, et al. Magnetic resonance spectroscopy metabolite profiles predict survival in paediatric brain tumors. Eur J Cancer 2013;49:457–64.

7. Jones C, Karajannis MA, Jones DTW, Kieran MW, Monje M, Baker SJ, et al. Pediatric high-grade glioma: Biologically and clinically in need of new thinking. Neuro Oncol 2017;19:153–61.

8. Jansen MHA, van Vuurden DG, Vandertop WP, Kaspers GJL. Diffuse intrinsic pontine gliomas: A systematic update on clinical trials and biology. Cancer Treat Rev 2012;38:27–35.

9. Hatae R, Hata N, Suzuki SO, Yoshimoto K, Kuga D, Murata H, et al. A comprehensive analysis identifies BRAF hotspot mutations associated with gliomas with peculiar epithelial morphology. Neuropathology 2017;37:191–9.

10. Korshunov A, Ryzhova M, Hovestadt V, Bender S, Sturm D, Capper D, et al. Integrated analysis of pediatric glioblastoma reveals a subset of biologically favorable tumors with associated molecular prognostic markers. Acta Neuropathol (Berl) 2015;129:669–78.

11. Mackay A, Burford A, Molinari V, Jones DTW, Izquierdo E, Brouwer-Visser J, et al. Profiling of non-brainstem pediatric high-grade molecular, pathological, radiological, and immune profiling of non-brainstem pediatric high-grade glioma from the HERBY Phase II Randomized Trial. Cancer Cell 2018:829–42.

12. Jaspan T, Morgan PS, Warmuth-Metz M, Sanchez Aliaga E, Warren D, Calmon R, et al. Response assessment in pediatric neuro-oncology: Implementation and expansion of the RANO criteria in a randomized phase II trial of pediatric patients with newly diagnosed high-grade gliomas. Am J Neuroradiol 2016;37:1581–7.

13. Wen PY, Macdonald DR, Reardon DA, Cloughesy TF, Sorensen AG, Galanis E, et al. Updated response assessment criteria for high-grade gliomas: Response assessment in neuro-oncology working group. J Clin Oncol 2010;28:1963–72.

14. Rodriguez D, Chambers T, Warmuth-Metz M, Aliaga ES, Warren D, Calmon R, et al. Evaluation of the implementation of the response assessment in neuro-oncology criteria in the HERBY trial of pediatric patients with newly diagnosed high-grade gliomas. AJNR Am J Neuroradiol 2019;40:568–75.

15. VASARI Project. (VASARI_MR_featurekey4.pdf).https://wiki.canceriamingarchive.net/display/Public/REMBRANDT. Accessed January 28, 2020.

16. Louis DN, Perry A, Reifenberger G, von Deimling A, Figarella-Branger D, Cavenee WK, et al. The 2016 World Health Organization classification of tumors of the central nervous system: a summary. Acta Neuropathol (Berl) 2016;131:803–20.

17. Schwartzentruber J, Korshunov A, Liu X-Y, Jones DTW, Pfaff E, Jacob K, et al. Driver mutations in histone H3.3 and chromatin remodelling genes in paediatric glioblastoma Jeremy. Nature 2012;482:226–31.

18. Wu G, Broniscer A, Mceachron TA, Lu C, Paugh BS, Becksfort J, et al. Somatic histone H3 alterations in pediatric diffuse intrinsic pontine. Nat Genet 2012;44:251–3.

19. Bender S, Tang Y, Lindroth AM, Hovestadt V, Jones DT, Kool M, et al. Article reduced h3k27me3 and dna hypomethylation are major drivers of gene expression in k27m mutant pediatric high-grade gliomas. Cancer Cell 2013;24:660–72.

20. Diaz AK, Baker SJ. The genetic signatures of pediatric high-grade glioma: no longer a one-act play. Semin Radiat Oncol 2014;24:240–7.

21. Aihara K, Mukasa A, Gotoh K, Saito K, Nagae G, Tsuji S, et al. H3F3A K27M mutations in thalamic gliomas from young adult patients. Neuro Oncol 2014;16:140–6.

22. Solomon DA, Wood MD, Tihan T, Bollen AW, Gupta N, Phillips JJJ, et al. Diffuse midline gliomas with histone H3-K27M mutation: a series of 47 cases assessing the spectrum of morphologic variation and associated genetic alterations. Brain Pathol 2016;26:569–80.

23. Louis DN, Giannini C, Capper D, Paulus W, Figarella-Branger D, Lopes MB, et al. cIMPACT-NOW update 2: diagnostic clarifications for diffuse midline glioma, H3 K27M-mutant and diffuse astrocytoma/anaplastic astrocytoma, IDH-mutant. Acta Neuropathol (Berl) 2018;135:639–42.

24. Aboian MS, Solomon DA, Felton E, Mabray MC, Villanueva-Meyer JE, Mueller S, et al. Imaging characteristics of pediatric diffuse midline gliomas with histone H3 K27M mutation. Am J Neuroradiol 2017;38:795–800.

25. Aboian MS, Tong E, Solomon DA, Kline C, Gautam A, Vardapetyan A, et al. Diffusion characteristics of pediatric diffuse midline gliomas with histone H3-K27M mutation using apparent diffusion coefficient histogram analysis. AJNR Am J Neuroradiol 2019;40:1804–10.

26. McCrea HJ, Bander ED, Venn RA, Reiner AS, Iorgulescu JB, Puchi LA, et al. Sex, age, anatomic location, and extent of resection influence outcomes in children with high-grade glioma. Neurosurgery 2015;77:443–53.

27. Finlay JL, Boyett JM, Yates AJ, Wisoff JH, Milstein JM, Geyer JR, et al. Randomized phase III trial in childhood high-grade astrocytoma comparing vincristine, lomustine, and prednisone with the eight-drugs-in-1-day regimen. Childrens Cancer Group. J Clin Oncol 1995;13:112–23.

28. Kang Y, Hong Choi S, Kim Y-J, Kim KG, Sohn CH, Kim JH, et al. Gliomas: histogram analysis of apparent diffusion coefficient maps with standard-or high-b -value diffusion-weighted mr imaging—correlation with tumor grade 1. Radiologyadiology 2011;261:882–90.

29. Kramm CM, Wagner S, Van Gool S, Schmid H, Sträter R, Gnekow A, et al. Improved survival after gross total resection of malignant gliomas in pediatric patients from the HIT-GBM studies 2006;3780:3773–9.

30. Karremann M, Gielen GH, Hoffmann M, Wiese M, Colditz N, Warmuth-Metz M, et al. Neuro-Oncology carry a dismal prognosis independent of tumor location. Neuro-oncol 2018;20:123–31.

31. Abbasi AW, Westerlaan HE, Holtman GA, Aden KM, van Laar PJ, van der Hoorn A. Incidence of tumor progression and pseudoprogression in high-grade gliomas: a systematic review and meta-analysis. Clin Neuroradiol 2018;28:401–11.

32. Sanghera P, Perry J, Sahgal A, Symons S, Aviv R, Morrison M, et al. Pseudoprogression following chemoradiotherapy for glioblastoma multiforme. Can J Neuro Sci 2010;37:36–42.

33. Radbruch A, Fladt J, Kickingereder P, Wiestler B, Nowosielski M, Baumer P, et al. Pseudoprogression in patients with glioblastoma: clinical relevance despite low incidence. Neuro-oncol 2015;17:151–9.

34. Balaña C, Capellades J, Pineda E, Estival A, Puig J, Domenech S, et al. Pseudoprogression as an adverse event of glioblastoma therapy. Cancer Med 2017;6:2858–66.

35. Parsa AT, Wachhorst S, Lamborn KR, Prados MD, McDermott MW, Berger MS, et al. Prognostic significance of intracranial dissemination of glioblastoma multiforme in adults. J Neurosurg 2005;102:622–8.

36. Arita N, Taneda M, Hayakawa T. Leptomeningeal dissemination if malignant gliomas. Incidence, diagnosis and outcome. Acta Neurochir (Wien) 1994;126:84–92.

37. Dardis C, Milton K, Ashby L, Shapiro W. Leptomeningeal metastases in high-grade adult glioma: Development, diagnosis, management, and outcomes in a series of 34 patients. Front Neurol 2014;5:1–10.

38. Wagner S, Benesch M, Berthold F, Gnekow AK, Rutkowski S, Sträter R, et al. Secondary dissemination in children with high-grade malignant gliomas and diffuse intrinsic pontine gliomas. Br J Cancer 2006;95:991–7.

39. Buczkowicz P, Bartels U, Bouffet E, Becher O, Hawkins C. Histopathological spectrum of paediatric diffuse intrinsic pontine glioma: diagnostic and therapeutic implications. Acta Neuropathol (Berl) 2014;128:573–81.